Electric field induced reorientation of polar molecules in a poly(methyl methacrylate) film studied by electroabsorption spectroscopy

Erko Jalviste*[a] and Nobuhiro Ohta*[b]

[a]Institute of Physics, University of Tartu, 142 Riia St., 51014 Tartu, Estonia
[b]Research Institute for Electronic Science (RIES), Hokkaido University, Sapporo 060-0812, Japan

ABSTRACT

Electroabsorption (EA) or Stark effect spectroscopy is a widely used method for characterizing the dopant molecules in polymer films and the films themselves. In this method the spectrum of a small (∼0.1%) absorbance change induced by a strong (∼1 MV/cm) electric field is measured. Analysis of the spectra provides information about the change in dipole moment and the change in polarizability accompanying an electronic transition. We measured near-UV absorption and EA spectra of indole-doped poly(methyl methacrylate) (PMMA) film prepared by a spin coating method. In the normal-incidence EA spectrum a negative contribution, being proportional to the absorption, was observed. In the case of magic angle between the electric vectors of the absorbed light and the applied field this contribution disappeared. These observations have been explained by field-induced orientation/alignment of the ensemble of polar indole molecules. Since the ground state dipole of indole is nearly parallel with the transition dipole, the absorption rate of light, which is polarized perpendicularly to the applied field, should be smaller. Our study demonstrated that the angular movement of indole-sized molecules in PMMA at room temperature is hindered, but not stopped.

Keywords: Spectroscopy, electroabsorption, Stark effect, alignment, orientation, angular distribution, PMMA, indole, electrostriction

1. INTRODUCTION

Doping a polymer with properly selected molecules is a common way for the creation of materials with desired properties for electro-optical applications, see e.g. Ref. 1 and references therein. The response of a doped polymer sample film to the externally applied electric field can be monitored optically by measuring the change in its absorbance, the change in its fluorescence,[2] the change in refraction index,[3] the second harmonic generation efficiency,[4] or the electrostrictive strain.[5] In the case of the Stark absorption (electroabsorption, EA) spectroscopy,[6–8] a small change in the absorption induced by an electric field is measured as a function of wavelength. The EA spectrum can be measured at different conditions, i.e., by varying the dopant concentration, the probe light incidence angle, the sample temperature, and the Stark alternation frequency.

The EA response of a guest-host polymer to the electric field depends on the electronic properties of individual dopant molecules (for instance, the energy level structure, the dipole moments and the polarizabilities in their ground and excited electronic states, the transition moment directions etc.) as well as their ensemble properties (for instance, the initial angular distribution of the dopant molecules and their reorientational mobility under the electric field) which are related to the relaxation properties of the host polymer. A host polymer is expected to be less rigid (the polymer relaxation is faster) at higher temperature (especially above its glass transition temperature T_g) and at higher concentration of the dopant or residual solvent molecules. For pure atactic PMMA, T_g is about 105 °C.[9] It should be noted that most detailed information about the polymer relaxation processes can be obtained by the dielectric measurements at different temperatures in a broad range of frequencies (from 0.1 Hz up to 1 MHz).[5, 10, 11]

*E.J.: E-mail: erko@fi.tartu.ee N.O.: E-mail: nohta@es.hokudai.ac.jp

Optical Materials and Applications, edited by Arnold Rosental, Proceedings of SPIE Vol. 5946
(SPIE, Bellingham, WA, 2005) · 0277-786X/05/$15 · doi: 10.1117/12.639175

The change in absorbance under an electric field can be divided into the components scaling linearly, quadratically, and as a higher power[12] with the field strength. If the initial angular distribution of guest molecules is *isotropic* the odd-order responses are suppressed and the lowest-order change in absorbance is quadratic to the applied field.[6] Experimentally, the quadratic EA response can be distinguished by using alternating Stark field and detecting the modulated EA signal at the second harmonic of the Stark alternation frequency.[6] At cryogenic temperatures, the mobility of guest molecules in a polymer is completely frozen so that (for non-poled samples) an isotropic and immobilized ensemble of molecules is formed. Such a conditions are ideal for probing the electronic properties of dopant molecules by (quadratic) EA spectroscopy. At higher temperatures polar molecules in a polymer environment can be (partially) reoriented by the electric field. In this case EA spectroscopy can provide information on the field-induced orientation and alignment of the guest molecules in the host polymer.

For the samples with frozen *anisotropic* orientational distribution of doped polar molecules, EA whose response is *linearly* proportional to the field strength appears because of nonequal number of blueshifting and redshifting molecules. An oriented and aligned ensemble of polar sample molecules can be prepared by poling the doped polymer under an electric field above its glass transition temperature and subsequent cooling the sample while keeping the poling field.[1, 13, 14] With a special technique, self-oriented monomolecular (Langmuir-Blodgett) layers can be prepared as a samples for linear EA spectroscopy.[2]

The observed quadratic EA spectra can be interpreted with the help of the Stark effect theory for solutions[6–8, 15] originally developed by Liptay and Czekalla.[16, 17] According to this theory the EA spectrum and the absorbtion spectrum of a given electronic transition are related to each other: the EA spectrum can be expressed as a linear combination of the zeroth, the first, and the second derivatives of the absorption spectrum. The coefficients of the linear combination depend on the parameters characterizing the dopant molecules (for instance, the change in dipole moment and the change in polarizability on electronic excitation) and on the parameters characterizing the experimental conditions (for instance, the temperature of the sample, the polarization and the incident angle of the probe light). Alternatively, the EA spectra can be interpreted using the concepts of nonlinear optics.[13, 18–21]

In a number of works[19, 20, 22–24] quadratic EA spectroscopy was used for the investigation of the field-induced reorientation (orientation and alignment) effects for an ensemble of dye molecules in a PMMA film. Saal and Haase[23] measured the EA spectra of Disperse Red 1 azo dye molecules, whose ground state dipole moment is 8.7 D, embedded into a spin-coated PMMA film. The ground state and the transition dipole moments of the dye were assumed to be parallel. The applied electric field was directed along the light propagation so that the light polarization makes a 90° with the direction of applied electric field. Measurements were performed at different sample temperatures and Stark field alternation frequencies ω. The analysis of $T = 105$ °C spectra revealed a transition from the mobile behavior at $\omega = 2$ Hz to immobile behavior at $\omega = 2$ kHz.

Chowdhury *et al.*[22] studied the EA spectra of Coumarin 153 ($\mu = 6.55$ D) in different host matrices at a magic angle condition between the light polarization and the applied field. The Stark field alternation frequency of 450 Hz was used. They found that the EA spectrum of the room-temperature PMMA samples depends strongly on the sample preparation method. For the samples heated (annealed) 5 minutes at 150 °C, the apparent measured polarizability change was about ten times smaller than for the samples dried for 24 hours at room temperature. This was explained by a smaller rigidity of unheated PMMA, which leads to the dominance of the field-induced dipolar orientation polarizability over the electronic polarizability change. Moreover, for frozen organic solvent hosts, the measured polarizability change was in turn an order of magnitude smaller, indicating that the embedded Coumarin 153 molecules are not completely immobilized at room temperature even for heated PMMA samples. Similar conclusions were in the EA study of all-trans retinal.[24]

In the present study, ultraviolet absorption and EA spectra of indole-doped PMMA are measured at a room temperature of 20 °C and at a cryogenic temperature of 53 K. Room-temperature spectra are measured at four different sample angles. Analysis of the absorption and EA data showed that the angular mobility of indole molecules is frozen at cryogenic temperature, but the embedded indole molecules are still partially reorientated by an electric field at room temperature. The choice of indole is justified by it small size, by its moderate dipole moment of 2.1 D in the ground state,[25] and by its importance as a chromophore of the amino-acid tryptophan.[26, 27] Although the overlapping of the electronic transitions in the UV region for indole complicates the data analysis,

Optical Materials and Applications, edited by Arnold Rosental, Proceedings of SPIE Vol. 5946
(SPIE, Bellingham, WA, 2005) · 0277-786X/05/$15 · doi: 10.1117/12.639175

most of the observed features in absorption and EA spectra are reproduced by a model simulation. Detailed discussion of the aspects related to the electronic properties of indole chromophore is published elsewhere.[28]

2. EXPERIMENTAL

For polarized EA measurements, the experimental set-up used in our previous EA studies[29–31] was complemented with a prism polarizer and a rotatable sample holder.

An indole-doped PMMA film was prepared by a spin coating method on a 20×60 mm^2 silica glass slide partially covered with a conductive indium-tin-oxide (ITO) layer. A solution for spin coating (indole and PMMA in benzene) with the indole/PMMA molar ratio (the number of moles of indole relative to the number of moles of PMMA monomer units) of 0.2 was prepared. After the spin coating, the sample slides were dried at room temperature about 24 hours and stored in a refrigerator in order to minimize the evaporation of indole out of the PMMA layer. The actual indole/PMMA molar ratio in the obtained PMMA layer (∼0.15) was estimated afterwards from the measured absorbance using the known molar extinction coefficient of indole. Indole (Tokyo Kasei Chemicals), 3-MI (Tokyo Kasei Chemicals), spectroscopic grade benzene (Waco Chemicals) and PMMA (Aldrich, MW=120000) were used without further purification. In order to avoid the evaporation of indole out of the PMMA layer, we did not heat (anneal) the sample.

The thickness of the indole-doped PMMA layer (typically about 0.5 μm) was measured with an interferometric microscope (NanoSpec/AFT 010-0180 from Nanometrics). The surface of the spin-coated PMMA layer had a rippling structure causing up to 100 nm variations in the local thickness value. Therefore, an average over 80-100 individual thickness measurements was calculated. After thickness measurements, a semitransparent aluminum film was vacuum-deposited on the indole-doped PMMA layer. ITO and aluminum layers were used as the Stark electrodes to which the wires were attached with a silver paste. The applied 40 Hz ac Stark voltage was set proportionally to the thickness of the sample film to ensure the same field strength of 1 MV/cm rms for different samples. Stronger electric field led to too often occurring breakthroughs.

Absorption spectra were measured with Hitachi U-3500 spectrometer using the spectral resolution of 1.5 nm. The absorption spectrum of indole was extracted by subtracting the measured spectrum of the sample slide, coated with a pure PMMA layer, from the measured spectrum of the same sample slide, coated with indole-doped PMMA. This procedure compensated the absorption of the ITO layer and eliminated the problem of larger reflection loss (∼0.06 O.D.) for bare ITO surface in comparison with the PMMA surface.

For room-temperature (T = 20 °C) polarized EA measurements, the converging light beam from JASCO FP777 fluorescence spectrometer was collimated with a pinhole (d = 1.4 mm) and a lens (f = 20 mm) and directed through a 10 mm-aperture α-BBO polarization prism (JDSU CASIX) and through the sample slide on an external photomultiplier. The pinhole and the lens confined the angular spread of the outcoming light within

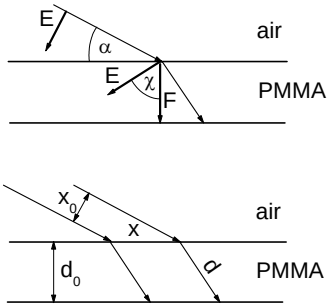

Figure 1. Upper panel illustrates the Snell's law relation between the angles α and χ, $\cos\alpha = n\cos\chi$, where α is the angle between the light beam and the sample slide and χ is the angle between the electric field vectors $\boldsymbol{E}$ (of the light) and $\boldsymbol{F}$ (of the applied field) in the PMMA layer. Lower panel explains the physical meaning of the quantities $1/\sin\chi = d/d_0$ and $1/\sin\alpha = x/x_0$, which describe the lengthening of the optical path in the PMMA layer and the lengthening of the light spot on the sample, respectively.

Optical Materials and Applications, edited by Arnold Rosental, Proceedings of SPIE Vol. 5946
(SPIE, Bellingham, WA, 2005) · 0277-786X/05/$15 · doi: 10.1117/12.639175

Table 1. Values of the relevant angle-dependent parameters at four different sample angles α used in the measurements. The physical meaning of χ, α, $1/\sin\chi$, and $1/\sin\alpha$ is illustrated in Fig. 1. The $3\cos^2\chi - 1 = 0$ condition defines the magic value of the χ angle. The refraction index of PMMA is assumed to be 1.544 at $\lambda = 270$ nm.[32]

$3\cos^2\chi - 1$	χ	α	$1/\sin\chi$	$1/\sin\alpha$
0.2	50.7°	12°	1.29	4.64
0	54.7°	27°	1.22	2.20
−0.5	65.9°	51°	1.09	1.29
−1	90°	90°	1	1

5° so that the allowed angular range of the polarization prism is not exceeded. A rotary stage was used for varying the angle between the sample slide and the light beam. The resolution of the spectrometer was set to 1.5 nm.

For low-temperature ($T = 53$ K) measurements, the sample was cooled with cryogenic refrigerating system (Daikin, V202C5LR). The temperature of the sample was monitored by a diode thermometer (Scientific Instruments, Si410A) connected to a temperature controller (Scientific Instruments, model 9600). The cryostat module was mounted either into the absorption spectrometer or into the EA spectrometer so that the probe light passed the cooled sample. All the low-temperature measurements were performed with a non-polarized light crossing the sample slide at normal incidence.

The signal from the photomultiplier was amplified and divided into two channels. The dc component reflecting the transmitted light intensity was recorded directly by a personal computer. The ac component was directed to a lock-in amplifier (SR830, SRS) detecting the signal at the second harmonic of the Stark field alternation frequency ω for the quadratic EA spectra. The amplitude and the phase signals from the output of the lock-in amplifier, which give the external field induced transmission change $\Delta I(\lambda, 2\omega)$, were digitized and recorded by a personal computer together with the dc component. To avoid the signal underflow or overflow in EA measurements the spectra were recorded in two parts, where the longer wavelength part was measured with a neutral attenuation filter, inserted into the path of the light beam.

The EA spectrum $\Delta A(\lambda) = A(\lambda, F) - A(\lambda, F = 0)$ was calculated from the measured ΔI and I spectra by[6, 15]

$$\Delta A(\lambda) = -(2\sqrt{2}/\ln 10)\Delta I(\lambda, 2\omega)/I(\lambda). \quad (1)$$

The factor $2\sqrt{2}$ converts the value of measured rms $\Delta I(\lambda, 2\omega)$ signal to its value as if measured with static Stark field and the factor $1/\ln 10$ comes from the definition of the absorbance, $A = -\log I/I_0$.

Room-temperature EA and absorption spectra were measured at four different angles α between the sample slide and the beam of the probe light, see Fig. 1 and Table 1. The selected α values correspond to the $3\cos^2\chi - 1$ factor of 0.2, 0, −0.5, and −1, where χ is the angle between the applied electric field $\boldsymbol{F}$ and the electric field of light $\boldsymbol{E}$ in the PMMA layer. For the light polarized in the incidence plane, the angles α and χ obey the Snell's law $\cos\alpha = n\cos\chi$, where n is the refraction index of PMMA. Its value, read out form the plot in Ref. 32, is 1.544 at 270 nm and 1.536 at 300 nm. The data in Table 1 were calculated using $n = 1.544$.

3. THEORY AND MODELING

The absorption spectrum of indoles in the near ultraviolet region of interest is formed by partially overlapped transitions from the ground state to the $\pi\pi^*$-type excited electronic states ^1L_a , ^1L_b , and ^1B_b . In the room-temperature solution spectra the ^1L_a band is stronger and less structured than the ^1L_b band. Owing to a larger permanent dipole moment in the ^1L_a state that that in the ^1L_b state, the ^1L_a absorption band is more redshifted in polar solvents than the ^1L_b band.[33]

It should be kept in mind that already the general electroabsorption theory[6–8] is based on several simplifying assumptions. (1) For individual molecules subjected to the electric field, the absorption band of a given electronic transition can shift in the frequency scale, but does not alter its shape. The apparent change of the band shape is

Optical Materials and Applications, edited by Arnold Rosental, Proceedings of SPIE Vol. 5946
(SPIE, Bellingham, WA, 2005) · 0277-786X/05/$15 · doi: 10.1117/12.639175

the result of ensemble average over the molecules experiencing different Stark shifts. (2) The absorption features are much broader than the Stark shift. (3) The angular distribution of molecules without the external field is isotropic. (4) The applied field is not too strong to induce orientational saturation i.e. $\mu F/kT \ll 1$. (5) The angular motion of the molecules is fast enough to follow a time-varying Stark field i.e. the angular distribution for an instantaneous field strength is the same as for a static field with the same strength. The opposite limit case of an immobile isotropically distributed ensemble of embedded molecules can be modelled by neglecting the orientation/alignment terms including the kT factor.

The absorption spectrum and the EA spectrum can be expressed as a sum of the contributions from participating electronic transitions to the ${}^1L_a$, ${}^1L_b$ and ${}^1B_b$ states,

$$A(\lambda,\chi) = (A^{\perp}_{La} + A^{\perp}_{Lb} + A^{\perp}_{Bb})(1/\sin\chi), \quad (2)$$

$$\Delta A(\lambda,\chi) = (\Delta A^{\chi}_{La} + \Delta A^{\chi}_{Lb} + \Delta A^{\chi}_{Bb})(1/\sin\chi), \quad (3)$$

where the symbol $\perp$ designates the absorbance at normal incidence condition, where χ=90°, and $1/\sin\chi$ is the optical path factor depending on the sample angle, see Fig. 1 and Table 1. The path factor $1/\sin\chi$ was assumed to be constant in the whole absorption range of indole and its value was taken from Table 1. The proportionality between the absorbance change ΔA and the path factor $1/\sin\chi$ can be rationalized as follows: the transmitted intensity I decreases proportionally to the optical path length, but the field-induced change of the transmitted intensity ΔI remains constant, since its increase is compensated by the decreased transmission.

In the electroabsorption model of indole further simplifying assumptions were introduced[28] in order to make feasible a least square model fit to the measured absorption and EA spectra. (1) Based on the available experimental[34] and *ab initio*[35] results, the change in permanent dipole moment is taken into account only for the ${}^1L_a \leftarrow S_0$ transition i.e. $\Delta\mu_{Lb} = 0$ and $\Delta\mu_{Bb} = 0$ were assumed. (2) For all three transitions, the polarizability anisotropy is neglected and the average polarizabilities are used for the characterization of the electronic states. (3) Based on the available *ab initio* results,[35,36] the ground state dipole $\boldsymbol{\mu}$ is assumed to be parallel with the ${}^1L_a \leftarrow S_0$ transition dipole $\boldsymbol{d}_{La}$. (4) The ${}^1L_b \leftarrow S_0$ transition dipole is assumed to be perpendicular to the ${}^1L_a \leftarrow S_0$ transition dipole. (5) The ground state dipole moment μ is fixed to its known value[25] of 2.09 D. (6) The internal field factor f whose typical values[6] range from 1.1 to 1.3 is assumed to be of 1.2.

The field induced change in absorbance for a given band, averaged over the angular distribution of molecules, can be then expressed as a sum of zeroth, first, and second derivatives by the frequency of the corresponding band shape as

$$\Delta A^{\chi}_{La} = (fF)^2 \left(a_{La} A^{\perp}_{La} + b_{La}\nu \frac{d(A^{\perp}_{La}/\nu)}{d\nu} + 1c_{La}\nu \frac{d^2(A^{\perp}_{La}/\nu)}{d\nu^2} \right), \quad (4)$$

$$\Delta A^{\chi}_{Lb} = (fF)^2 \left(a_{Lb} A^{\perp}_{Lb} + b_{Lb}\nu \frac{d(A^{\perp}_{Lb}/\nu)}{d\nu} \right), \quad (5)$$

$$\Delta A^{\chi}_{Bb} = (fF)^2 \left(b_{Bb}\nu \frac{d(A^{\perp}_{Lb}/\nu)}{d\nu} \right), \quad (6)$$

where f is the internal field factor taking into account the local field in the cavity where the molecule is placed[8] and F is the strength of the applied electric field. According to the assumptions described above the coefficients which depend on the angle χ can be expressed as

$$a_{La} = (q_2^2\mu^2/15k^2T^2)(3\cos^2\chi - 1), \quad (7)$$

$$b_{La} = \Delta\alpha_{La}/2h + (q_1\mu\Delta\mu_{La}/3hkT)\cos\gamma + (2q_1\mu\Delta\mu_{La}/15hkT)\cos\gamma(3\cos^2\chi - 1), \quad (8)$$

$$c_{La} = \Delta\mu^2_{La}/6h^2 + (\Delta\mu^2_{La}/30h^2)(3\cos^2\gamma - 1)(3\cos^2\chi - 1), \quad (9)$$

$$a_{Lb} = -(q_2^2\mu^2/30k^2T^2)(3\cos^2\chi - 1), \quad (10)$$

$$b_{Lb} = \Delta\alpha_{Lb}/2h, \quad (11)$$

$$b_{Bb} = \Delta\alpha_{Bb}/2h, \quad (12)$$

where μ is the dipole moment in the ground electronic state, $\Delta\mu_{La}$ and $\Delta\mu_{La}$ are the change in the dipole moment and $\Delta\alpha_{La}$ and $\Delta\alpha_{Lb}$ are the change in average polarizability on corresponding transitions, $\chi = \boldsymbol{E}\angle\boldsymbol{F}$ is the angle

Optical Materials and Applications, edited by Arnold Rosental, Proceedings of SPIE Vol. 5946
(SPIE, Bellingham, WA, 2005) · 0277-786X/05/$15 · doi: 10.1117/12.639175

between polarization direction of the absorbing light and the applied electric field, $\gamma = \mathbf{\Delta\mu}_{La} \angle \boldsymbol{\mu} = \mathbf{\Delta\mu}_{La} \angle \boldsymbol{d}_{La}$, and kT is the Boltzmann factor. The empirical parameters q_1 and q_2, whose values are between 0 and 1, are introduced to take into account the restricted mobility of indole molecules in PMMA.

The zeroth-derivative contribution to the absorption change of the ${}^1L_a$ band, i.e. the $(fF)^2 a_{La} A_{La}^{\perp}$ factor in Eq. (4), arises from the deviation of the distribution of the ensemble of transition dipoles from isotropy owing to the alignment of the ground state dipoles along the field direction. (The transition dipole is assumed to be not influenced by the electric field.) For an ensemble of molecules with parallel ground state and transition dipoles, the electric field being parallel (perpendicular) to the probe light polarization leads to the increased (decreased) absorbtion.

In the first- and second-derivative contributions, the electronic response of a molecule to the applied field appears through the field-induced Stark shift of the transition frequencies,

$$h\Delta\nu_{La} = -\Delta\mu_{La} fF - (1/2)\Delta\alpha_{La}(fF)^2, \quad (13)$$

$$h\Delta\nu_{La} = -(1/2)\Delta\alpha_{Lb}(fF)^2, \quad (14)$$

$$h\Delta\nu_{Bb} = -(1/2)\Delta\alpha_{Bb}(fF)^2. \quad (15)$$

Thus, the first-derivative contribution for the ${}^1L_a$ band, $(fF)^2 b_{La}\nu[d(A_{la}^{\perp}/\nu)/d\nu]$, arises from the Stark shift of the absorption band owing to the polarizability change and by the concerted effect of the field-induced orientation of the ground state dipoles and the linear Stark shift, see Eq. (8). For an orientated ensemble, where the number of molecules with redshifted absorption band is larger than the number of molecules with blueshifted band, the ensemble average results in an effective redshift. We note that the orientation component of the field induced distribution function alone cannot cause a change in absorbance, because the increase in a number of dipoles in the vicinity of a selected direction is compensated with equal decrease in the vicinity of the opposite direction.

The second-derivative contribution for the ${}^1L_a$ band, i.e. $(fF)^2 c_{La}\nu[d^2(A_{La}^{\perp}/\nu)/d\nu^2]$, arises from the apparent field-induced broadening of the shape of the absorption band owing to the ensemble average of different dipole-induced Stark shifts $\langle\Delta\nu^2\rangle$ [Eq. (13)] of individual molecules. Non-zero ensemble-averaged $\langle\Delta\nu^2\rangle$, but zero-valued $\langle\Delta\nu\rangle$ follows from equal number of molecules with blueshifted and redshifted absorption band. Here the angular distribution of molecules is assumed to be isotropic. Field-induced orientation/alignment coupled with the Stark effect gives rise to the higher order terms and does not contribute to the second-derivative term.

Equations (1-12) provide a link between the microscopic parameters characterizing the molecule and its environment ($\Delta\alpha_{La}$, $\Delta\mu_{La}$, $\cos\gamma$, $\Delta\alpha_{Lb}$, $\Delta\alpha_{Bb}$, q_1, q_2) and the measured quantities ($A(\lambda)$, F, χ, $I(\lambda)$, $\Delta I(\lambda)$, and T). Apart from the seven listed parameters, the shapes of the ${}^1L_a$, ${}^1L_b$, and ${}^1B_b$ absorption bands have to be determined. A least square fitting routine was used to vary the fit parameters until the best match between the calculated and the observed spectra was achieved. The shapes of the absorption bands were modeled as a sum of Gaussian functions, where a single Gaussian describes the rising edge of the ${}^1B_b$ band, three Gaussians describe the ${}^1L_a$ band and two Gaussians describe the ${}^1L_b$ band.[28]

The spectra measured at $T = 53$ K were visually compared with the simulated ones, but not quantitatively fitted. The simulated 53 K absorption spectrum was assumed to be the same as the room-temperature spectrum obtained from the fit. The 53 K EA spectrum was simulated by neglecting all the dipole orientation terms in Eqs. (7) and (8), which contain the Boltzmann factor. This takes into account that the orientations of embedded molecules are fixed at a cryogenic temperature. The remaining non-zero coefficients are

$$b_{La} = \Delta\alpha_{La}/2h, \quad (16)$$

$$c_{La} = \Delta\mu_{La}^2/6h^2 + (\Delta\mu_{La}^2/30h^2)(3\cos^2\gamma - 1)(3\cos^2\chi - 1), \quad (17)$$

$$b_{Lb} = \Delta\alpha_{Lb}/2h, \quad (18)$$

$$b_{Bb} = \Delta\alpha_{Bb}/2h. \quad (19)$$

4. RESULTS AND DISCUSSION

Measured and simulated room-temperature absorption spectra of indole are shown in Fig. 2(a). Only the normal-incidence-case ($\alpha = \chi = 90^\circ$) spectra are shown. The other three spectra observed at the sample angle α smaller

Optical Materials and Applications, edited by Arnold Rosental, Proceedings of SPIE Vol. 5946
(SPIE, Bellingham, WA, 2005) · 0277-786X/05/$15 · doi: 10.1117/12.639175

than 90° had the same shape, and their scaling factors ($1/\sin\chi$) agreed with the predicted ones given in Table 1 within 10%. The quadratic EA spectra measured at normal incidence ($\alpha = \chi = 90°$) and at the magic angle ($\alpha = 27°$ and $\chi = 55°$) are shown in Figs. 2(b). The EA curve for $\chi = 66°$ lies between the curves for $\chi = 55°$ and $\chi = 90°$, and the EA curve for $\chi = 51°$ lies above the curve for $\chi = 55°$. The absorption and the EA spectrum of indole measured at a temperature of 53 K at $\chi = 90°$ are shown in Fig. 3(a) and Fig. 3(b), respectively.

Some conclusions can be made immediately from the observed EA spectra shown in Figs. 2(b) and 3(b). (1) In the room-temperature normal-incidence EA spectrum the decrease in absorbance in the region of the absorption maximum is clearly dominating over the small increase in absorbance in the low-frequency part. This decrease in absorbance must be caused by a non-vanishing zeroth-derivative contribution for some electronic transition since the first-derivative and the second-derivative contributions integrated over spectral range covering the whole band, must cancel out. (2) in the magic-angle room-temperature spectrum and in the normal-incidence 53 K spectrum, the decrease and the increase in absorbance seem to be balanced. (3) the amplitude of the EA signal in the 53 K spectrum is much smaller than in the room-temperature spectrum. As shown below, the observed effects can be explained in terms of the field-induced orientation/alignment of embedded polar indole molecules in PMMA environment at room temperature.

The molecular parameters of indole determined from the model fit to the room-temperature spectra are listed in Table 2. With these parameters, the measured absorption and EA spectra are reproduced reasonably well by a simulation as shown in Figs. 2(a), 2(b), 3(a), and 3(b). Figures 2(a) and 3(a) also show the shapes of the ${}^1B_b$, ${}^1L_a$, and ${}^1L_b$ bands, from which the simulated absorption spectra are composed of. The decomposition of the simulated EA spectra of indole to the ${}^1B_b$, ${}^1L_a$, and ${}^1L_b$ constituents, is shown in Figs. 2(c) and 3(c) in the normal incidence ($\chi = 90°$) case and in Figs. 2(d) in the magic angle ($\chi = 55°$) case.

The b_{La} coefficient [Eq. (8)] can be written as

$$b_{La} = \Delta\alpha_{La}^{eff}(\chi)/2h, \tag{20}$$

where

$$\Delta\alpha_{La}^{eff}(\chi) = \Delta\alpha_{La} + (2q_1\mu\Delta\mu_{La}/3kT)\cos\gamma + (4q_1\mu\Delta\mu_{La}/15kT)\cos\gamma(3\cos^2\chi - 1) \tag{21}$$

is the apparent (effective) polarizability change, which includes the electronic polarizability change as well as the dipolar orientational (the orientational polarizability) contribution.

The $\Delta\alpha_{La}^{eff}(\chi)$ values are given in Table 2 for the magic angle case, where $\chi = 54°$ and $3\cos^2\chi - 1 = 0$, and for the normal incidence case, where $\chi = 90°$ and $3\cos^2\chi - 1 = -1$, are given in Table 2. Larger value of $\Delta\alpha_{La}^{eff} - \Delta\alpha_{La}$ in comparison with that of $\Delta\alpha_{La}$ indicates that in the room-temperature EA spectra the dipolar orientational contribution to the first-derivative b_{La} term is dominating in the room-temperature EA spectra. About twice larger magnitude of the first-derivative b_{La} component in the magic angle case than that in the normal incidence case (compare Fig. 2(d) with Fig. 2(c)) follows from the χ-dependence of the orientational polarizability and the optical path factor $1/\sin\chi$.[28] Much ($\Delta\alpha/\Delta\alpha_{La}^{eff}(90°) = 0.22$ times) smaller first-derivative ${}^1L_a$ component in the cryogenic EA spectrum is a direct consequence of the absence of orientational effects at low temperatures.

Considering that the angular dependence of the energy of a dipole in an electric field is given by $-\mu F\cos(\boldsymbol{\mu}\angle\boldsymbol{F})$ the *equilibrium* angular distribution function for an ensemble of (ground state) dipoles in the electric field at a temperature T and its expansion to the Legendre polynomials (in the orientationally unsaturated case where $\beta = \mu F/kT \ll 1$) can be written as

$$W(\theta) = \exp(\beta\cos\theta) \approx 1 + \beta P_1(\theta) + (1/3)\beta^2 P_2(\theta), \tag{22}$$

where $\theta = \boldsymbol{\mu}\angle\boldsymbol{F}$. The Legendre polynomials $P_0(\theta) = 1$, $P_1(\theta) = \cos\theta$, and $P_2(\theta) = (3/2)\cos^2\theta - 1/2$ describe the isotropic, the *orientation*, and the *alignment* contribution to the angular distribution function, respectively. The degree of *orientation* can be characterized by the ensemble average of "cosine theta", $\langle\cos\theta\rangle$, being equal to $(1/3)\beta$ in case of $\beta \ll 1$. The alignment-type deviation from isotropy, proportional to F^2, gives rise to the zeroth-derivative term in the EA theory [Eq. (7)] and the orientation-type deviation from isotropy, proportional to F, gives rise to the first-derivative term [Eq. (8)].

Optical Materials and Applications, edited by Arnold Rosental, Proceedings of SPIE Vol. 5946
(SPIE, Bellingham, WA, 2005) · 0277-786X/05/$15 · doi: 10.1117/12.639175

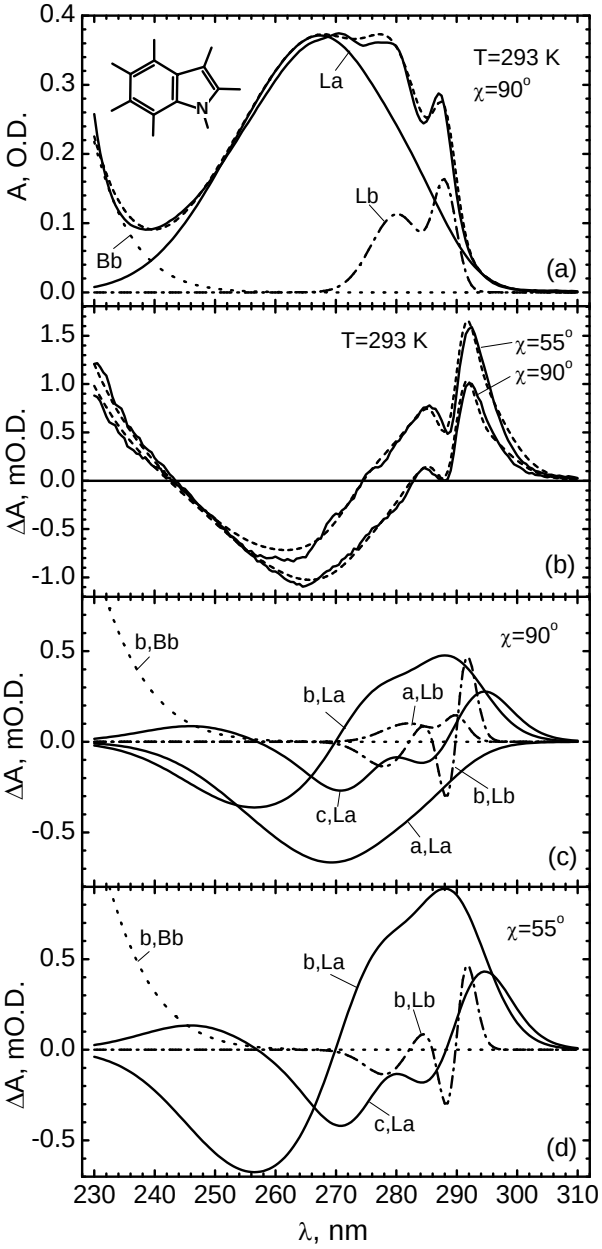

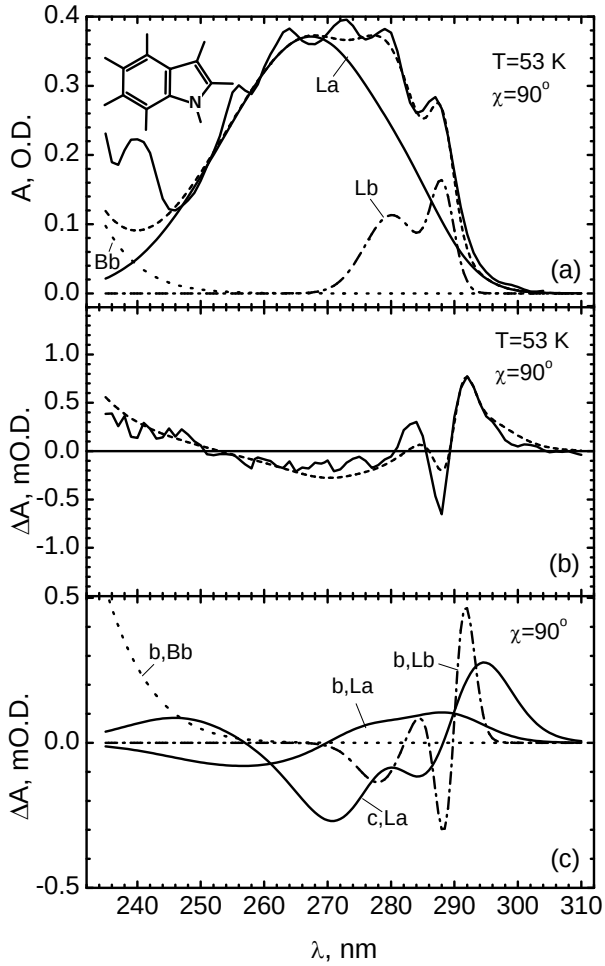

Figure 2. Room-temperature spectra of indole in PMMA: (a) observed (solid curve) and simulated (dashed curve) absorption spectrum and its decomposition to the ^1L_a , ^1L_b , and ^1B_b bands (labeled curves); (b) observed (solid curves) and simulated (dashed curves) EA spectra in the magic angle case and in the normal incidence case; (c) the a_{La}, b_{La}, c_{La}, a_{Lb}, b_{Lb}, and b_{Bb} components of the simulated EA spectrum in the normal incidence case; (d) the b_{La}, c_{La}, b_{Lb}, and b_{Bb} components in the magic angle case. The letters a, b, and c designate the zeroth-, the first-, and the second-derivative contributions, respectively.

Figure 3. Spectra of indole in PMMA at T=53 K: (a) observed absorption spectrum (solid curve), simulated absorption spectrum (dashed curve) and its decomposition to the ^1L_a , ^1L_b , and ^1B_b bands (labeled curves); (b) observed (solid curves) and simulated (dashed curves) electroabsorption (EA) spectra for indole in the normal incidence case ($\chi = 90^\circ$); (c) the b_{La}, c_{La}, b_{Lb}, and b_{Bb} components of the simulated EA spectrum. The letters b and c designate the first-, and the second-derivative contributions, respectively. The absorbance and its change is given in dimensionless optical density units.

Optical Materials and Applications, edited by Arnold Rosental, Proceedings of SPIE Vol. 5946
(SPIE, Bellingham, WA, 2005) · 0277-786X/05/$15 · doi: 10.1117/12.639175

Table 2. Molecular parameters from the model fit to the measured absorption and electroabsorption spectra of indole. The reported values are corrected by the internal field factor $f = 1.2$. The ground state dipole moment μ was fixed to 2.1 D in the fit. See Sec. 3 for the definition of the parameters.

$\Delta\mu_{La}$	4.7	D
$\Delta\alpha_{La}$	9	Å^3
$\Delta\alpha_{Lb}$	13	Å^3
q_2	0.56	
q_1/q_2	0.72	
γ	34	deg
$\Delta\alpha_{La}^{eff}(55°)$	63	Å^3
$\Delta\alpha_{La}^{eff}(90°)$	41	Å^3

According to Eq. (22), low temperature should favor the orientation/alignment owing to the $\beta = \mu F/kT$ factor. This is indeed true in case of fast relaxation to the equilibrium angular distribution at a given field strength and temperature. Actually, the mobility of an indicator molecule and its local polymer surrounding, resulting in the field-induced orientation/alignment, is suppressed at low temperatures. Intuitively, higher mobility and consequently faster equilibration of the angular distribution is expected for lower Stark field alternation frequency, for a less rigid host polymer, and for smaller size of embedded molecules. A host polymer is expected to be less rigid at higher temperature (especially above its glass transition temperature) and at higher concentration of the dopant molecules.

The actual (unrelaxed) angular distribution of dopant dipoles, which follows the time-varying electric field only partially, can be described as[23, 28]

$$W(\theta)^{eff} = 1 + q_1\beta P_1(\theta) + (1/3)q_2^2\beta^2 P_2(\theta), \tag{23}$$

where the empirical parameters $q_1(\omega, T)$ and $q_2(\omega, T)$ depend on the field alternation frequency ω and the sample temperature T. Through the distribution function $W(\theta)^{eff}$ the q_1 and q_2 factors appear in Eqs. (7) and (8). In the limit of a mobile ensemble of dipoles, whose distribution follows the field in a full extent, $q_1 = q_2 = 1$. In the opposite limit of a spatially fixed isotropic ensemble $q_1 = q_2 = 0$.

The q_2 value of 0.56 (Table 2) indicates, that the alignment of indole molecules to the instantaneous strength of the 40 Hz ac field is partial. This means that the mobility of indole is significantly restricted by the surrounding PMMA environment. The q_2 coefficient can also be regarded as a ratio of apparent and real ground state dipole moments. The inequality $q_1/q_2 < 1$ indicates that in our experimental conditions ($\omega = 40$ Hz and $T = 20$ °C) the orientation component of the apparent field-induced angular distribution is suppressed in relation to the alignment component.

In the transparency region of the sample (from 300 nm to 600 nm), the normal incidence EA spectrum of some sample showed a periodic sine-like modulation around the zero level, whose amplitude was of ∼0.1 mO.D.. A constant-frequency interval between the adjacent maxima (∼5500 cm^{-1}) indicates that the modulation is caused by the thin-film interference effect. Obviously, electrostrictive strain[3, 5, 37, 38] of the dopant/PMMA layer being proprortional to the square of the applied electric field is responsible for the field-induced frequency shift of the modulation pattern in transmitted intensity giving rise to its appearance in the EA spectrum.

5. SUMMARY

Room-temperature ultraviolet absorption and electroabsorption (EA) spectra of indole-doped PMMA film are measured under different angles between the the polarization direction of the light and the applied electric field direction. Low-temperature ($T = 53$ K) EA measurements, where the indole molecules in PMMA are doubtlessly immobilized, confirmed that polar molecules tend to reorientate themselves along to the electric field direction

Optical Materials and Applications, edited by Arnold Rosental, Proceedings of SPIE Vol. 5946
(SPIE, Bellingham, WA, 2005) · 0277-786X/05/$15 · doi: 10.1117/12.639175

in room-temperature PMMA. The measured spectra were reproduced by a model simulation taking into account three overlapped electronic transitions of indole and the field-induced alignment/orientation effects.

Field-induced dipolar *alignment* appeared in the room temperature normal incidence EA spectra as an absorbance decrease, whose spectrum is proportional to the ^1L_a absorption spectrum. Since for indole the ground state dipole moment and the $^1L_a \leftarrow S_0$ transition dipole moment are almost parallel, the aligned ensemble of molecular dipoles absorbs the light, which is polarized perpendicularly to the applied field, less than the isotropic ensemble.

About twice smaller dipolar alignment contribution, than expected on the basis of the known value of the ground state dipole moment indicated that the angular mobility of indole is significantly restricted by the PMMA host matrix. In other words, the orientational relaxation of indole in a PMMA matrix at room temperature is too slow for the angular distribution of the ground state molecular dipoles to follow in a full extent the instantaneous strength of the 40 Hz ac Stark field.

Field-induced dipolar *orientation* appeared in the room-temperature EA spectra through the temperature and sample angle dependent redshift of the absorption band. In the magic angle case, the apparent polarizability change on $^1L_a \leftarrow S_0$ excitation, which includes both the electronic and the dipolar orientation contribution, was 6-7 times larger than the electronic polarizability change $\Delta\alpha_{La}$.

ACKNOWLEDGMENTS

E. J. is thankful to the Japan Society for the Promotion of Science (JSPS) for funding his research stay in Hokkaido Univerity. This work was supported by Grants-in-Aid for Scientific Research (A) (2) (15205001) and for Scientific Research on Priority Area (417) from the Ministry of Education, Culture, Sports, Science and Technology of Japan.

REFERENCES

1. F. Ghebremichael, M. G. Kuzyk, and H. S. Lackritz, "Nonlinear optics and polymer physics." http://www.usafa.af.mil/dfp/research/lorc/polymer/all_rev/, 1997.
2. N. Ohta, "Electric field effects on photochemical dynamics in solid films," *Bull. Chem. Soc. Jpn.* **75**, pp. 1637–1655, 2002.
3. F. Ghebremichael and H. S. Lackritz, "Improved interferometer studies of linear electro-optic effects of dye-doped polymers," *Appl. Opt.* **36**, pp. 4081–4089, 1997.
4. G. T. Boyd, C. V. Francis, J. E. Trend, and D. A. Ender, "Second-harmonic generation as a probe of rotational mobility in poled polymers," *J. Opt. Soc. Am. B* **8**, pp. 887–894, 1991.
5. H.-J. Winkelhahn, T. Pakula, and D. Neher, "Investigation of the viscoelastic properties of thin polymer films by electromechanical interferometry," *Macromolecules* **29**, pp. 6865–6871, 1996.
6. G. U. Bublitz and S. G. Boxer, "Stark spectroscopy: applications in chemistry, biology and materials science," *Annu. Rev. Phys. Chem.* **48**, pp. 213–242, 1997.
7. W. Liptay, "Dipole moments and polarizabilities of molecule in excited electronic states," in *Excited States, vol. 1*, E. C. Lim, ed., pp. 129–229, Academic Press, New York, 1974.
8. M. Ponder and R. Mathies, "Excited-state polarizabilities and dipole moments of diphenylpolyens and retinal," *J. Phys. Chem.* **87**, pp. 5090–5098, 1983.
9. F. W. J. Billmeyer, *Textbook of Polymer Science*, John Wiley and Sons, New York, 1984.
10. K. Fukao, S. Uno, Y. Miyamoto, A. Hoshino, and H. Miyaji, "Dynamics of α and β processes in thin polymer films: poly(vinyl acetate) and poly(methyl methacrylate)," *Phys. Rev. E* **64**, pp. 51807–51817, 2001.
11. D. Lei, J. Runt, and R. E. Newnham, "Dielectric properties of azo dye-poly(methyl methacrylate) mixtures," *Macromolecules* **20**, pp. 1797–1801, 1987.
12. K. Lao, L. J. Moore, H. Zhou, and S. G. Boxer, "Higher-order Stark spectroscopy: polarizability of photosynthetic pigments," *J. Phys. Chem.* **99**, pp. 496–500, 1995.
13. C. Heldmann, L. Brombacher, D. Neher, and M. Graf, "Dispersion of the electro-optical response in poled polymer films determined by Stark spectroscopy," *Thin Solid Films* **265**, pp. 241–247, 1995.

Optical Materials and Applications, edited by Arnold Rosental, Proceedings of SPIE Vol. 5946
(SPIE, Bellingham, WA, 2005) · 0277-786X/05/$15 · doi: 10.1117/12.639175

14. T. Goodson and C. H. Wang, "Dispersion and dipolar orientation effects on the linear electroabsorption and electro-optic responses in a model quest/host nonlinear optical system," *J. Appl. Phys.* **80**, pp. 6602–6609, 1996.
15. S. A. Locknar and L. A. Peteanu, "Investigation of the relationship between dipolar properties and cis-trans configuration in retinal polyenes: a comparative study using Stark spectroscopy and semiempirical calculations," *J. Phys. Chem. B* **102**, pp. 4240–4246, 1998.
16. W. Liptay and J. Czekalla, "Die Bestimmung von absoluten Übergangsmomentrichtungen und von Dipolmomenten angeregter Moleküle aus Messugen des elektrischen Dichroismus. I. Theorie," *Z. Naturforsch. A* **15**, pp. 1072–1079, 1960.
17. W. Liptay and J. Czekalla, "Die Beeinflussung der optischen Absorption von Molekülen durch ein äußeres elektrisches Feld. Erweiterte Theorie," *Z. Electrochem. Ber. Bunsenges. Phys. Chem.* **65**, pp. 721–727, 1961.
18. S. Umeuchi, Y. Nishimura, I. Yamazaki, H. Murakami, M. Yamashita, and N. Ohta, "Electric field effects on absorption and fluorescence spectra of pyrene doped in a PMMA polymer film," *Thin Solid Films* **311**, pp. 239–245, 1997.
19. C. Poga, M. G. Kuzyk, and C. W. Dirk, "Quadratic electroabsorption studies of third-order susceptibility in dye-doped polymers," *J. Opt. Soc. Am. B* **11**, pp. 80–91, 1994.
20. C. Poga, T. M. Brown, M. G. Kuzyk, and C. W. Dirk, "Characterization of the excited states of a squaraine molecule with quadratic electroabsorption spectroscopy," *J. Opt. Soc. Am. B* **12**, pp. 531–543, 1995.
21. K. D. Singer, M. G. Kuzyk, and J. E. Sohn, "Second-order nonlinear-optical processes in orientationally ordered materials: relationship between molecular and macroscopic properties," *J. Opt. Soc. Am. B* **4**, pp. 968–976, 1987.
22. A. Chowdhury, S. A. Locknar, L. L. Premvardhan, and L. A. Peteanu, "Effects of matrix temperature and rigidity on the electronic properties of solvatochromic molecules: electroabsorption of Coumarin 153," *J. Phys. Chem. A* **103**, pp. 9614–9625, 1999.
23. S. Saal and W. Haase, "Relaxation phenomena in polymeric guest-host systems studied by stark spectroscopy (electroabsorption)," *Chem. Phys. Lett.* **278**, pp. 127–132, 1997.
24. S. A. Locknar, A. Chowdhury, and L. A. Peteanu, "Matrix and temperature effects on the electronic properties of conjugated molecules: An electroabsorption study of *all-trans*-retinal," *J. Phys. Chem. B* **104**, pp. 5816–5824, 2000.
25. W. Caminati and S. Di Bernardo, "Microwave spectrum and amino hydrogen location in indole," *J. Mol. Struct.* **240**, pp. 253–262, 1990.
26. P. R. Callis and B. K. Burgess, "Tryptophan fluorescence shifts in proteins from hybrid simulationa: an electrostatic approach," *J. Phys. Chem. B* **101**, pp. 9429–9432, 1997.
27. D. W. Pierce and S. G. Boxer, "Stark effect spectroscopy of tryptophan," *Biophys. J.* **68**, pp. 1583–1591, 1995.
28. E. Jalviste and N. Ohta, "Stark spectroscopy of indole and 3-methylindole," *J. Chem. Phys.* **121**, pp. 4730–4739, 2004.
29. N. Ohta, S. Okazaki, and I. Yamazaki, "Stark shift in absorption spectra of Langmuir-Blodgett mixed monolayer films. new finding of a complex formation of chromophoric oxacyanine," *Chem. Phys. Lett.* **229**, pp. 394–400, 1994.
30. N. Ohta, T. Ito, S. Okazaki, and I. Yamazaki, "External electric field effects on absorption and fluorescence spectra of monomer and dimer of oxacarbocyanine in Langmuir-Blodgett films," *J. Phys. Chem. B* **101**, pp. 10213–10220, 1997.
31. N. Ohta, Y. Iwaki, T. Ito, I. Yamazaki, and A. Osuka, "Photoinduced charge transfer along a *meso,meso*-linked porphyrin array," *J. Phys. Chem. B* **103**, pp. 10242–10245, 1999.
32. T. A. Osswald and G. Menges, *Materials Science of Polymers*, Hanser, Munich, 1996.
33. H. Lami and N. Glasser, "Indole's solvatocromism revisited," *J. Chem. Phys.* **84**, pp. 597–604, 1986.
34. C.-T. Chang, C.-Y. Wu, A. R. Muirhead, and J. R. Lombardi, "The dipole moment in the lowest singlet $\pi^* \leftarrow \pi$ state of indole determined by the optical Stark effect," *Photochem. Photobiol.* **19**, pp. 347–351, 1974.

Optical Materials and Applications, edited by Arnold Rosental, Proceedings of SPIE Vol. 5946
(SPIE, Bellingham, WA, 2005) · 0277-786X/05/$15 · doi: 10.1117/12.639175

35. A. L. Sobolewski and W. Domcke, "Ab initio investigations on the photophysics of indole," *Chem. Phys. Lett.* **315**, pp. 293–298, 1999.
36. L. Serrano-Andrés and B. Roos, "Theoretical study of the absorption and emission spectra of indole in the gas phase and in a solvent," *J. Am. Chem. Soc.* **118**, pp. 185–195, 1996.
37. R. E. Newnham, V. Sundar, R. Yimnirun, J. Su, and Q. M. Zhang, "Electrostriction: nonlinear electromechanical coupling in solid dielectrics," *J. Phys. Chem. B* **101**, pp. 10141–10150, 1997.
38. M. G. Kuzyk, J. E. Sohn, and C. W. Dirk, "Mechanism of quadratic electro-optic modulation of dye-doped polymer systems," *J. Opt. Soc. Am. B* **7**, pp. 842–858, 1990.

Optical Materials and Applications, edited by Arnold Rosental, Proceedings of SPIE Vol. 5946
(SPIE, Bellingham, WA, 2005) · 0277-786X/05/$15 · doi: 10.1117/12.639175